RAPID COMMUNICATIONS

PHYSICAL REVIEW B VOLUME 49, NUMBER 10 1 MARCH 1994-II

Energy transfer from tetrahedral Fe^{3+} sites to Tm^{3+} in garnets

V. Lupei and A. Lupei
Institute of Atomic Physics, 76900 Bucharest, Romania

G. Boulon, A. Brenier, and C. Pedrini
Laboratoire de Physico-Chimie des Materiaux Luminescents, Université Claude Bernard Lyon, 69622 Villeurbanne, France

M. J. Elejalde
Escuela Technica Superior de Ingenieros Industriales de Telecomunicacion, Universidad del Pais Vasco, 48013 Bilbao, Spain
(Received 14 September 1993; revised manuscript received 22 December 1993)

A very efficient energy transfer from Fe^{3+} (d tetrahedral sites) to Tm^{3+} (c dodecahedral sites) in yttrium aluminum garnet and gadolinium gallium garnet crystals was observed. The site-selective spectroscopy shows that in case of near-neighbor Fe(d)-Tm pairs the transfer efficiency is 100%. For the other pairs it is less efficient and increases with temperature due to a better superposition of Fe^{3+} emission and $^3H_4$ Tm^{3+} absorption bands.

Energy transfer from transition-metal ions to Tm^{3+} in garnets is the subject of an intense investigation in view of sensitization of the two-micron laser emission of this ion. The previous studies refer to $3d$ ions that occupy the octahedral a sites in these crystals. On the other hand, sensitization with transition-metal ions in tetrahedral sites seems attractive for several reasons. First, the number of tetrahedral sites near the dodecahedral c sites occupied by Tm^{3+} is larger than that of octahedral sites and the shortest sensitizator-activator distance is smaller. Second, the inversionless symmetry of the tetrahedral sites allows electric and magnetic transitions between the states of the ground $3d^n$ configuration and this assures strong absorptions and an efficient energy transfer.

The aim of this paper is the investigation of energy transfer from Fe^{3+} in tetrahedral sites to Tm^{3+} in gadolinium gallium garnet (GGG) and yttrium aluminum garnet (YAG) crystals. Fe^{3+} could occupy either the octahedral a or tetrahedral d sites in garnets, the site preference depending on the actual composition of the crystal.[1] Besides the above advantages of the sensitizer in the d sites, it is also known from magnetic studies that stronger superexchange interactions exist between rare earths in c sites and $Fe^{3+}(d)$ ions. The emission spectrum of Fe^{3+} in tetrahedral sites matches very well the absorption of the $^3H_4$ Tm^{3+} level.[2,3] Under these circumstances an effective energy transfer to this Tm^{3+} level takes place, as our preliminary investigations have shown.[4]

The crystals used in this investigation (YAG or GGG with Fe concentrations up to 1 at.% and Tm up to 5 at.%) have been grown by pulling from melt in iridium crucibles and in a slightly oxidizing atmosphere to reduce the formation of Fe^{2+} centers.

The $3d^5$ ground configuration of Fe^{3+} contains a spin sextet ^6S, the ground term, four spin quartets ($^4P, ^4D, ^4F, ^4G$) and several spin doublets. The intermediate cubic field component (of T_d symmetry) at the tetrahedral site splits the free-ion terms of the $3d^5$ configuration according to the Tanabe-Sugano diagram (Fig. 1). For Fe^{3+} in tetrahedral sites the ratio Dq/B is usually close to one. Additional splittings of the cubic crystal-field states are due to the spin-orbit coupling, thus $^6A_1 \rightarrow \Gamma_7 + \Gamma_8$, $^4A_{1,2} \rightarrow \Gamma_8$, $^4E \rightarrow \Gamma_6 + \Gamma_7 + \Gamma_8$, $^4T_{1,2} \rightarrow \Gamma_6 + \Gamma_7 + 2\Gamma_8$. The low symmetry component of crystal field could split the Γ_8 quartets into doublets. For the Fe^{3+} in octahedral sites the Tanabe-Sugano diagram is similar, but the Dq/B is usually slightly larger than two.

In a cubic field the transitions between the ground state and the excited states are forbidden, both by spin and parity. The spin forbiddeness, at least for transitions between the spin sextet and spin quartet states, is lessened by the spin-orbit mixing. For the tetrahedral center the parity forbiddeness is largely removed by the upper configurations mixing into the ground $3d^5$ configuration, determined by the odd crystal-field components. Thus spin-flip optical absorption from the sextet ground state (the splitting of the ground state, as EPR data have shown, is of the order of several 10^{-2} cm^{-1} and can be disregarded from an optical point of view) to the upper spin quartet crystal-field split levels is possible.[5-7] For Fe^{3+} a-octahedral isolated centers the inversion symmetry is preserved so no electric dipole transitions could be expected, unless low symmetry perturbations occur.

The optical absorption spectra in our crystals show mostly contribution from tetrahedral Fe^{3+} centers; the

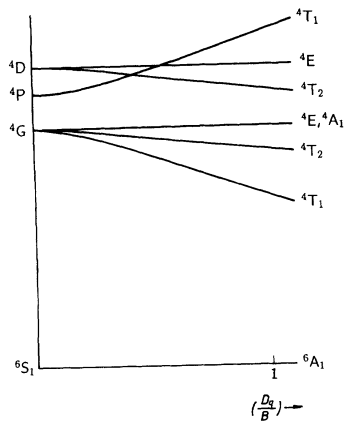

FIG. 1. Tanabe-Sugano diagram for Fe^{3+} in cubic tetrahedral field.

lines are usually broad and weak especially on the long wavelengths. However, previous studies[5–7] on various iron garnets, where Fe^{3+} occupies both the tetrahedral and octahedral sites have shown transitions of considerable intensity. For the tetrahedral centers these spectra extend from about 750–760 nm to uv, while for octahedral centers the lowest energy absorption lies in the 1000 nm range. A very strong line (peaking at 255 nm in YAG) was assigned to charge-transfer transitions inside both the tetrahedral and octahedral Fe^{3+} centers.

An interesting feature of the $Fe^{3+}(d)$ optical spectra in garnets is the presence of a strong and sharp zero-phonon line into $^4T_2(^4D)$, accompanied by a phonon side-band with unresolved structure. This line peaks at 421.16 nm in GGG [Fig. 2(a)], while in YAG it is resolved into two components (414.12 and 414.27 nm) due to the spin-orbit splitting [$\Gamma_8(5/2)$ and Γ_6 components] of $^4T_2$. In both these crystals a broad absorption corresponding to the $^6A_1 - ^4T_2(^4G)$ transition is observed in the 530 nm region so that the crystals can be pumped by the second harmonic of the YAG:Nd laser.

By excitation in the $3d$ intraconfiguration absorption lines or in the charge transfer band, $Fe^{3+}(d)$ shows luminescence only from the first excited $^4T_1(^4G)$ level to the $^6A_1$ ground state. This luminescence depends on the host crystal and on temperature. In YAG at very low temperatures (5 K) a sharp and intense zero-phonon line at 763.1 nm, accompanied by a weak phonon sideband peaking around 781.5 nm is observed. With increasing temperature, several other zero-phonon lines show up, first at 762.5 then at 760.5 nm, their intensity being correlated with the thermal population of the spin-orbit components of the emitting level. At the same time the phonon sideband broadens and gains in intensity; at room temperature it dominates the emission and extends up to about 850 nm, with the maximum around 780 nm. In the case of GGG, the Fe^{3+} emission consists, at 5 K, of a group of three relatively sharp lines at 753.3, 754.8, and 756.8 nm accompanied by a phonon sideband stronger than in YAG [Fig. 3(a)]. The origin of this triplet is not clear: since the temperature dependence of the intensity cannot be correlated with the large splittings, the lines could not be assigned to the spin-orbit structure of the emitting or ground levels. Thus other models such as a preferential electron-phonon coupling or a magnetic interaction between Fe^{3+} with the Gd^{3+} sublattice should be considered. At room temperature, as for YAG, the emission is dominated by the phonon sideband that peaks in the 770–785 nm range and extends up to 840–850 nm.

The luminescence decay of 0.5 at. % Fe-doped YAG or GGG is exponential with a time decay parameter depending on temperature: at 300 K this is about 7.5 ms in YAG and 4.5 ms in GGG. Together with the strong phonon sideband, this suggests a stronger electron-phonon coupling for Fe^{3+} in the second crystal. As shown by EPR measurements and optical studies on concentrated crystals, part of Fe^{3+} could enter in octahedral a sites. Though no absorption or emission lines connected with $Fe^{3+}(a)$ centers could be observed in our spectra,

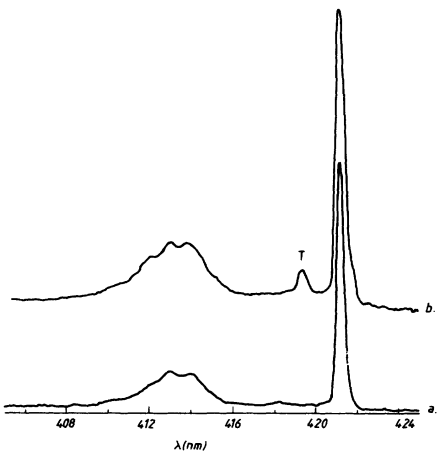

FIG. 2. Optical absorption spectrum, $^6A_1 \rightarrow ^4T_2(^4D)$ Fe^{3+} transition, at 5 K for (a) GGG:Fe(0.5 at. %) and (b) GGG:Fe(0.5 at. %):Tm(5 at. %).

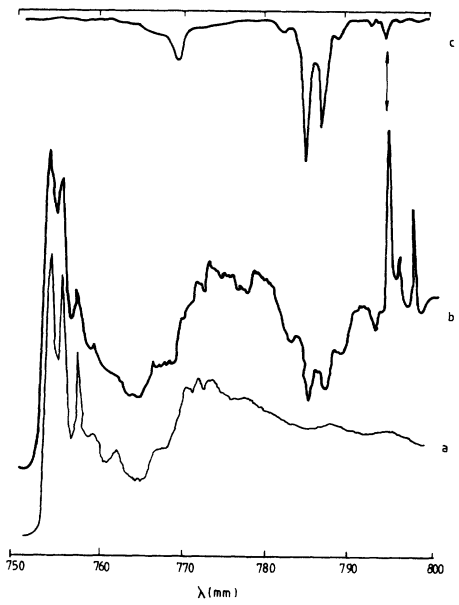

FIG. 3. Emission spectrum at 10 K of a GGG:Fe(0.5 at. %) (a), of a GGG:Fe:Tm sample (b) showing dips that correspond to Tm^{3+} absorption (c).

they could influence the dynamic behavior of $Fe^{3+}(d)$ emission. The Fe^{3+} decay are quasiexponential, independent of Fe content (up to 1%) in single doped samples. On the other hand, the excitation spectra of $Fe^{3+}(d)$ and of Tm^{3+} $^3H_4$ emission (in YAG:Fe,Tm) do not show any line which could be assigned to $Fe^{3+}(a)$. This indicates no energy transfer from $Fe^{3+}(a)$ to $Fe^{3+}(d)$ or to Tm $^3H_4$ levels; however, such a transfer would be possible to Tm levels lower than the lowest excited level of $Fe^{3+}(a)$, such as $^3H_5$.

The co-doping with Tm^{3+} has influence on the spectroscopic properties of Fe^{3+} in garnets; the most evident effect is the presence of resolved satellites near the $^6A_1 \rightarrow {}^4T_2(^4D)$ transition. Such a satellite (T) is observed at 419.56 nm for GGG [Fig. 2(b)], while in YAG two satellites at 413.94 and 413.77 nm (i.e., split by about 9–10 cm^{-1} as the spin-orbit components of the main line) show up. The intensities of these satellite lines could be correlated with Tm^{3+} concentration C. The relative intensity of the satellite line T to the main $Fe^{3+}(d)$ absorption line [Fig. 2(b)] in a GGG sample co-doped with 5 at. % Tm^{3+} is about 0.1 and this equals the value $2C(1-C)$ predicted by the statistical distribution of Tm^{3+} ions in one of the two nearest-neighbor c sites around $Fe^{3+}(d)$, for a random distribution of dopants. This fact suggests that the satellite T corresponds to a nearest-neighbor $Fe^{3+}(d)$-Tm^{3+} pair. A similar situation holds for YAG. Unfortunately, due to the large width of the lines, similar satellites could not be resolved in other absorption transitions of $Fe^{3+}(d)$.

Co-doping with Fe and Tm of YAG and GGG induces satellite lines in the Tm^{3+} absorption spectra. Since the Tm^{3+} lines are much sharper, a richer structure of satellites with intensities increasing with Fe and Tm content could be observed. For the elucidation of Fe-Tm energy transfer processes, the analysis of Fe^{3+} emission characteristics at selective excitation is important.

By excitation in the main sharp lines of the $^6A_1 \rightarrow {}^4T_2(^4D)$ transition in co-doped samples, the normal $Fe^{3+}(d)$ emission spectra is obtained by with several dips in the emission phonon sidebands, their contour following closely the line shape of the $^3H_6 \rightarrow {}^3H_4$ Tm^{3+} absorption spectra, as can be seen in Fig. 3 for GGG. These dips show that a radiative energy transfer from Fe^{3+} in d sites to Tm^{3+} could take place. At the same time the Fe^{3+} luminescence decay is strongly changed: it shows marked nonexponentialities, proportional to the Tm^{3+} concentration (as illustrated in Fig. 4 for YAG). This is an indication that nonradiative transfer from $Fe^{3+}(d)$ to Tm^{3+} takes place, too. A similar behavior of decay is observed by nonselective pumping with the second harmonic of a YAG:Nd laser. At long times after the laser pulse, the Fe^{3+} decay can be described by a Förster $\gamma t^{1/2}$ law, with γ proportional to the Tm^{3+} concentration. This corresponds to a dipole-dipole interaction between distant Fe-Tm ions; this interaction cannot, however, describe the beginning of the decay. This could be an indication that stronger Fe-Tm coupling might occur in the closer pairs. The analysis of the decay is complicated by the lack of any $Fe^{3+}(d)$ emission at pumping in T-type satellites. This shows that in the

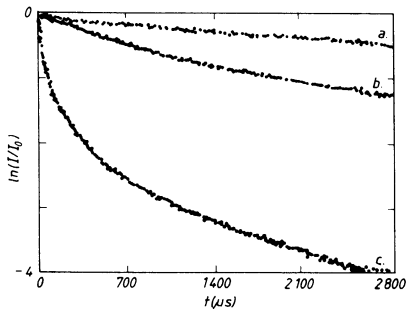

FIG. 4. Luminescence decays of Fe^{3+} in YAG at 300 K for (a) YAG:Fe(0.5 at. %); (b) YAG:Fe(0.5 at. %):Tm(1 at. %); (c) YAG:Fe(0.5 at. %):Tm(5 at. %).

$Fe^{3+}(d)$-Tm^{3+} pair, corresponding to the T satellite, the transfer is so strong that it quenches completely the Fe^{3+} luminescence.

The $Fe^{3+}(d)$-Tm^{3+} energy transfer is also evident in Tm^{3+} emission by pumping selectively in the T satellite or at various wavelengths inside the $^6A_1 \rightarrow {}^4T_2$ absorption line. The emission (at low temperatures) depends on the pump wavelength and on Fe and Tm concentrations and contain several new lines, not observed in Tm^{3+} single doped crystals. The ensemble of all these new lines could be observed also by pumping nonselectively with the second harmonic of the YAG:Nd laser. Three main new emission lines (F_1, F_2, and F_3) have been observed in the $^3H_4$ emission both in GGG [with the $^3H_4(W_1) \rightarrow {}^3H_6(Z_1)$ transition at 795.33, 795.29, and 795.05 nm, as compared with the normal emission N at 794.98 nm] and YAG (794.71, 793.98, and 793.07 nm, as compared to 793.5 nm$-N$ line). Evidently these satellites correspond to various short distance Fe(d)-Tm(c) pairs. The $^3H_4 \rightarrow {}^3H_6$ emission spectra for F_i centers contain more lines than Tm^{3+} in normal c^- sites. In D_2 local symmetry of c sites the crystal-field components of Tm^{3+} are split in singlets that could be labeled by the four irreducible representations Γ_i and the $\Gamma_i \rightarrow \Gamma_i$ optical transitions are forbidden.[2] Such a restriction does not exist for any group of symmetry lower than D_2. The perturbation produced by $Fe^{3+}(d)$ at the Tm^{3+} site in the near pairs lowers the symmetry, making thus all the optical transitions allowed. Richer optical spectra are indeed observed for the new F_i centers. A significant illustration of this effect is the presence of the $W_1 \rightarrow Z_2$ transition that in D_2 symmetry is forbidden.[2] By contrast, strong such lines (F_1', F_2' in Fig. 5) are observed for centers F_1 and F_2, that are the most shifted from the line N, but not for F_3 that is closer to N. These perturbations could also alter to a considerable extent the probabilities for all the transitions.

The most shifted satellite in Tm^{3+} emission (F_1) could be excited by pumping in the satellite T of Fe^{3+} absorption; this suggests that they correspond to the same Fe(d)-Tm(c) formation. The strong spectral shifts of these satellites coupled with the 100% efficient energy transfer from Fe to Tm for this center indicate that it should correspond to the nearest-neighbor $Fe^{3+}(d)$-Tm pair. According to the relative positions of $Fe^{3+}(d)$ and

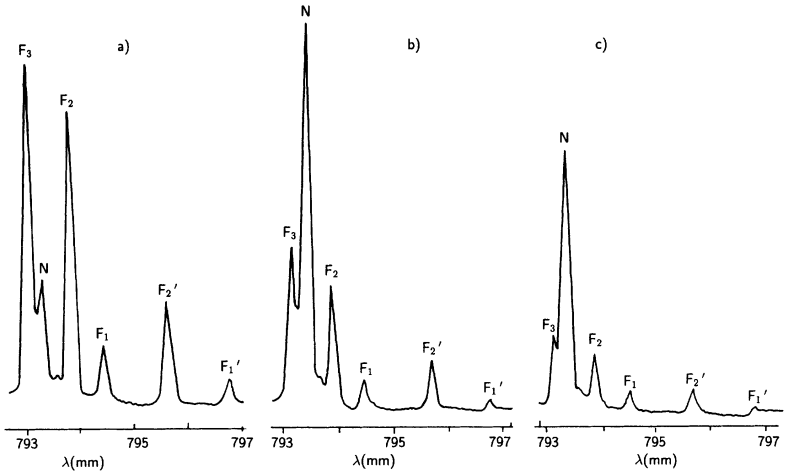

FIG. 5. Part of the $^3H_4 \rightarrow {}^4H_6$ Tm^{3+} emission in YAG:Fe(0.5 at. %):Tm(5 at. %) under nonselective excitation with 532 nm in Fe^{3+}, registered at different delay times: (a) 0 μs, (b) 200 μs, (c) 800 μs.

Tm^{3+} in the crystalline lattice for this pair the perturbation produced by $Fe^{3+}(d)$ at the Tm^{3+} site would lower the crystal-field symmetry from D_2 to C_2 and this produces the observed alteration of selection rules and oscillator strengths.

The luminescence decays of the F_1, F_2, and F_3 satellites are similar, but they differ from the decay of the Tm^{3+} emission at the main center N wavelength that presents a noticeable concentration and temperature-dependent rise time. This shows that for the F_1, F_2, and F_3 centers, that correspond to close Fe(d)-Tm pairs, the coupling between ions is very strong and thus the transfer from Fe to Tm is very fast; by contrast, for more distant pairs, where the crystal-field perturbation is weak and no shift occurs, the interaction is weaker and thus a clear rise time is observed. This is clearly illustrated by time-resolved emission spectroscopy. Figure 5 shows the $^3H_4 \rightarrow {}^3H_5$ emission spectra in the region of $W_1 \rightarrow Z_1$ and $W_1 \rightarrow Z_2$ transitions for a YAG:Fe(1%):Tm(1%) at 10 K registered at various delays from 532 nm laser exciting pulse. Another feature of this emission must be stressed: when pumping nonselective in Fe^{3+}, the $^3H_4$ emission of Tm^{3+} is dominated by the three new centers F_1, F_2, and F_3 and this effect increases with Fe and Tm concentration. The large transfer efficiency within these pairs and their increased concentration at larger dopants content could explain this effect. The $^3H_4$ emission quenching by cross relaxation and reabsorption effects could also influence the spectra.

The impossibility to fit the beginning of luminescence decay both for donors and acceptors in these systems shows that the energy transfer rate for several near pairs is larger than predicted by the dipolar interaction with the microparameter C_{DA} determined from long-time behavior of decay. There are several possible reasons: (i) a larger microparameter C_{DA} for dipolar interaction, due to a better superposition of Fe emission and Tm absorption for these pairs; this could be due to the richer absorption Tm spectrum for these lower symmetry centers. (ii) the onset of higher-order multipolar interaction for closer pairs. (iii) a contribution from strong, short-distance superexchange interaction between $Fe^{3+}(d)$ and Tm^{3+}.

We note also that the efficiency of $Fe^{3+}(d)$-Tm^{3+} transfer increases with temperature. This could be connected with a better superposition of Fe^{3+} emission with Tm^{3+} absorption at elevated temperatures.

In conclusion, a very efficient energy transfer from Fe^{3+} in tetrahedral d sites to the $^3H_4$ level of Tm^{3+} takes place. The site selective excitation due to the resolution of satellites in the absorption spectrum of Fe^{3+} and in the emission spectrum of Tm^{3+} enables a characterization of the transfer inside the various Fe(d)-Tm pairs; this transfer is very efficient (100% in the case of nearest pairs which produces the satellites F_1, F_2, and F_3 in Tm emission), it is governed by a multiple interaction picture for the next closer pairs, and it is dipolar for more distant pairs. The efficiency of transfer increases with temperature due to a better superposition of Fe^{3+} emission sideband and of $^3H_4$ Tm^{3+} absorption. Due to a combined static (crystal-field perturbation) -dynamic (larger transfer rate for the short distance Fe-Tm pairs) effect, the spectral composition of $^3H_4$ emission is modified by this sensitization. The investigation of the effect of this selective transfer on the two-micron emission of Tm^{3+} is in progress.

[1]P. Röschmann, J. Phys. Chem. Solids **41**, 569 (1980).
[2]J. B. Gruber *et al.*, Phys. Rev. B **40**, 9464 (1989).
[3]A. Lupei *et al.*, J. Appl. Phys. (to be published).
[4]V. Lupei *et al.*, in *Solid State Lasers IV*, edited by Gregory J. Quarles and M. A. Woodall, SPIE Proceedings Vol. 1864 (SPIE, Bellingham, WA, 1993).
[5]P. Kohler and G. Amthauer, J. Solids Chem. **28**, 329 (1979).
[6]J. C. Canit *et al.*, Solid State Commun. **42**, 653 (1982).
[7]Yu. A. Voitukevich *et al.*, Opt. Spectrosc. **63**, 480 (1987).